AMERICAN SOCIETY FOR MICROBIOLOGY | Journal of Bacteriology®

RESEARCH ARTICLE

BosR Is A Novel Fur Family Member Responsive to Copper and Regulating Copper Homeostasis in *Borrelia burgdorferi*

Peng Wang,[a] Zhuoteng Yu,[a] Thomas J. Santangelo,[b] John Olesik,[c] Yufeng Wang,[d] Ekaterina Heldwein,[e] Xin Li[a]

Division of Geographic Medicine and Infectious Diseases, Tufts Medical Center, Boston, Massachusetts, USA[a]; Department of Biochemistry and Molecular Biology, Colorado State University, Fort Collins, Colorado, USA[b]; Trace Element Research Laboratory, The Ohio State University, Columbus, Ohio, USA[c]; Department of Biology, University of Texas at San Antonio, San Antonio, Texas, USA[d]; Department of Molecular Biology and Microbiology, Tufts University School of Medicine, Boston, Massachusetts, USA[e]

ABSTRACT The ferric uptake regulator (Fur) family of DNA-binding proteins represses and/or activates gene transcription via divalent metal ion-dependent signal sensing. The *Borrelia burgdorferi* Fur homologue, also known as *Borrelia* oxidative stress regulator (BosR), promotes spirochetal adaptation to the mammalian host by directly repressing the lipoproteins required for tick colonization and indirectly activating those required for establishing infection in the mammal. Here, we examined whether the DNA-binding activity of BosR was regulated by any of the four most prevalent transition metal ions in *B. burgdorferi*, Mn, Fe, Cu, and Zn. Our data indicated that in addition to a structural site occupied by Zn(II), BosR had two regulatory sites that could be occupied by Zn(II), Fe(II), or Cu(II) but not by Mn(II). While Fe(II) had no effect, Cu(II) and Zn(II) had a dose-dependent inhibitory effect on the BosR DNA-binding activity. Competition experiments indicated that Cu(II) had a higher affinity for BosR than Zn(II) or Fe(II). A BosR deficiency in *B. burgdorferi* resulted in a significant increase in the Cu level but no significant change in the levels of Mn, Fe, or Zn. These data suggest that Cu regulates BosR activity, and BosR in turn regulates Cu homeostasis in *B. burgdorferi*. While this regulatory paradigm is characteristic of the Fur family, BosR is the first one shown to be responsive to Cu(II), which may be an adaptation to the potentially high level of Cu present in the Lyme disease spirochete.

IMPORTANCE Transition metal ions serve an essential role in the metabolism of all living organisms. Members of the ferric uptake regulator (Fur) family play critical roles in regulating the cellular homeostasis of transition metals in diverse bacteria, and their DNA-binding activity is often regulated by coordination of the cognate divalent metal ions. To date, regulators with metal ion specificity to Fe(II), Mn(II), Zn(II), and Ni(II) have all been described. In this study, we demonstrate that BosR, the sole Fur homologue in *Borrelia burgdorferi*, is responsive to Cu(II) and regulates Cu homeostasis in this bacterium, which may be an adaption to potentially Cu-rich milieu in the Lyme disease spirochete. This study has expanded the repertoire of the Fur family's metal ion specificity.

KEYWORDS *Borrelia burgdorferi*, *Borrelia* oxidative stress regulator, DNA-binding protein, copper, ferric uptake regulator, fluorescence anisotropy, metalloregulation

Received 26 April 2017 **Accepted** 1 June 2017

Accepted manuscript posted online 5 June 2017

Citation Wang P, Yu Z, Santangelo TJ, Olesik J, Wang Y, Heldwein E, Li X. 2017. BosR is a novel Fur family member responsive to copper and regulating copper homeostasis in *Borrelia burgdorferi*. J Bacteriol 199:e00276-17. https://doi.org/10.1128/JB.00276-17.

Editor Richard L. Gourse, University of Wisconsin—Madison

Address correspondence to Xin Li, xli4@tuftsmedicalcenter.org.

Lyme disease is the most common vector-borne disease in the Northern Hemisphere (1, 2). The causative agent, *Borrelia burgdorferi sensu lato*, is maintained in an enzootic cycle consisting of an *Ixodes* tick vector and a small vertebrate reservoir

host, often a rodent (3). Successful adaptation to these vastly different niches by the spirochete requires differential gene expression (4, 5). Studies have shown that *Borrelia* oxidative stress regulator (BosR) plays a critical role in spirochetal adaptation to the mammalian host environment, during which BosR directly represses the expression lipoproteins required for colonization of the tick, such as outer surface protein A (OspA) (6), and indirectly activates the RpoS-dependent expression of lipoproteins required for infection of the mammal, such as OspC (7, 8).

BosR is a member of the ferric uptake regulator (Fur) family of DNA-binding proteins. Fur was first described in *Escherichia coli* as a repressor of ferric uptake, because its absence resulted in constitutive expression of several proteins involved in ferric iron uptake even under iron-replete conditions (9). Further characterization of Fur revealed a DNA-binding protein that required Fe(II) as a cofactor to bind to and repress transcription from target promoters (10). To date, Fur homologues have been found in diverse Gram-negative and Gram-positive bacteria, and some have different metal ion specificities from that of Fur (11). The zinc-responsive Zur, the manganese-responsive Mur, and the nickel-responsive Nur all have been shown to regulate the homeostasis of their respective metal ions in a manner similar to that of Fur (12–15). There are also examples of Fur-like proteins sensing metal-dependent but nonmetal signals, including the *Bacillus subtilis* peroxide regulon repressor (PerR), which senses peroxide stress through Fe(II)-catalyzed oxidation of a proximal histidine residue (16), and the *Bradyrhizobium japonicum* iron-responsive regulator (Irr), which senses iron availability through direct binding of heme, the end product of a biosynthesis pathway that utilizes iron (17).

There is a great level of diversity in the regulatory mechanisms of various Fur family members. In the case of *E. coli* Fur, coordination of Fe(II) is thought to induce conformational changes which enhance its DNA-binding activity, thus allowing repression of iron uptake genes under iron-replete conditions. While Fe(II) is believed to be the regulatory metal ion of Fur *in vivo*, other divalent metal ions, such as Mn(II), Co(II), and Cd(II), can functionally replace Fe(II) in *in vitro* DNA-binding assays (10). Although Fur was first recognized as a repressor, examples of Fur-activating transcription, either directly or indirectly, have also been reported (11, 18). In the case of Irr and PerR, signal sensing by these regulators leads to either protein degradation or a reduction in DNA-binding activity, therefore resulting in derepression or activation of gene expression (16, 17).

Genes targeted by the Fur family of metalloregulators are not limited to those involved in maintaining metal ion homeostasis. Many Fur homologues have been shown to be global regulators that affect metabolism, motility, stress responses, biofilm formation, and pathogenicity (19–24). While most Fur family members recognize palindromic DNA sequences that follow the 7-1-7 rule (i.e., a 1-bp spacer separating a pair of 7-bp palindromic sequences) (11, 23), variations to this rule have been reported (6, 25). Two recent genome-wide studies of *Campylobacter jejuni* and *E. coli* Fur regulons suggest that the consensus sequences targeted for activation could differ significantly from those targeted for repression and may not even be palindromic (22, 24).

To date, a total of 21 crystal structures have been reported for 12 members of the Fur family (22, 25–38). With the exception of the *E. coli* Fur structure, which is of an amino-terminal truncate, all the other structures are of full-length proteins. Notably, structures of the *E. coli* Zur and the *Magnetospirillum gryphiswaldense* Fur are solved in complex with target DNA molecules, offering insights into DNA recognition by the Fur family of regulators (36, 38). All structures indicate that members of the Fur family of regulators exist as homodimers, with each subunit consisting of two distinct domains, an amino-terminal DNA-binding domain (DBD) and a carboxyl-terminal dimerization domain (DD), connected by a flexible hinge region. The relative position of the DBD to the DD, however, varies significantly among these structures, with some structures in a conformation capable of binding to DNA, also known as the closed form, and others in the so-called open form, being incapable of binding to DNA (36). Transition from the open form to the closed form requires significant conformational changes that bring

the DBDs from two monomers closer to each other so that both can make contact with DNA.

The greatest level of diversity among these structures stems from the sites of metal ion coordination. While none of these metal-binding sites identified by crystallography is conserved in all structures, three of them are common to multiple structures (see Fig. S1 in the supplemental material). The least variable of these three sites involves a tetrahedral coordination of a Zn(II) ion by four cysteines, which are contributed by two CXXC motifs in the DD. This site, sometimes known as site 1 (S1), is thought to play a structural role, because it is important for maintaining the dimer formation (28, 34, 36). The other two sites, sometimes known as sites 2 and 3 (S2 and S3, respectively), are often assigned a regulatory role, meaning that metal ion coordination at these sites can trigger conformational changes that affect the DNA-binding activity of the protein.

BosR is the only Fur homologue encoded by the *B. burgdorferi* genome (39). Phylogenetic analysis of BosR and the 12 Fur family members with available crystal structures indicates that BosR is more closely related to the PerR orthologs from *B. subtilis* and *Streptococcus pyogenes* than to the Fur or the Zur orthologs from various bacteria (Fig. S2). Of the three common metal ion-binding sites described in other Fur family members, only S1, the site composed of four cysteines, appears to be conserved in BosR (Fig. S1 and S3). The absence of S2 and S3 in BosR raises interesting questions regarding metalloregulation of BosR. Is the DNA-binding activity of BosR regulated by divalent metal ions like other Fur family members? Does metalloregulation of BosR employ novel metal ion-binding sites? There have been precedents of novel metal ion-binding sites: the Ni(II)-coordinating site in *Streptomyces coelicolor* Nur and the Ni(II)/Zn(II)-coordinating site in *S. pyogenes* PerR both appear to be unique to themselves (Fig. S1). Notably, BosR has an extended amino terminus, as well as an extended carboxyl terminus, which could provide a structural basis for novel metal ion-binding sites (Fig. S1).

Despite an increasing appreciation of the critical role of BosR in the *B. burgdorferi* life cycle (7, 8, 40), there has not been a consensus on whether or how this putative metalloregulator may be regulated by metal ions (41, 42). Two recent studies have prompted us to reexamine the metalloregulation of BosR. First, new BosR targets have been identified in *B. burgdorferi*, and the consensus BosR-binding sequence is proposed to follow the 7-(0, 2)-7 rule, whereby the spacer between the pair of 7-bp palindromic sequences varies from 0 to 2 bp in length (6). Although two earlier studies on BosR metalloregulation used the promoter region of *bb0690* as the target DNA, data from this recent study indicated that BosR bound to the *ospAB* promoter with a much higher affinity than to the *bb0690* promoter (6). Second, in addition to Zn and Mn, Fe and Cu have been identified as transition metal ions that might be present in *B. burgdorferi* at $>10^5$ atoms/cell (43). Here, we examined whether Zn, Mn, Fe, or Cu was capable of binding to BosR and whether these metal ions affected the DNA-binding activity of BosR using the BosR-binding site identified in the *ospAB* promoter. We also investigated whether BosR played any role in maintaining metal ion homeostasis in *B. burgdorferi*.

RESULTS

BosR has a structural Zn(II) site. Recombinant BosR was affinity purified from *E. coli* to apparent homogeneity as a soluble His_6-tagged protein, and the tag was then cleaved off as described previously (see Fig. S4 in the supplemental material and Materials and Methods for details) (6). The molecular mass of the tag-free BosR was estimated to be 37.6 kDa by size-exclusion chromatography, which corresponds to a dimer (Fig. S5). Zinc, detected by inductively coupled plasma-sector field mass spectrometry (ICP-SFMS), is the only metal that was consistently present at a significant level in the recombinant tag-free BosR. The Zn levels in four different preparations of BosR were 0.98, 1.48, 1.72, and 1.82 atoms per BosR dimer, indicating that BosR, as isolated, contained up to two atoms of Zn per dimer. Despite variations in the Zn level, these different preparations of BosR showed no significant differences in DNA-binding activity (data not shown).

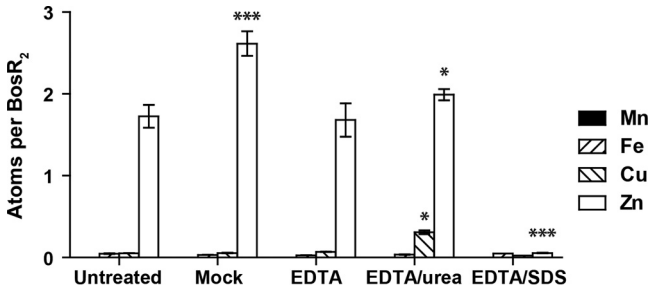

FIG 1 Recombinant BosR contains a structural Zn site. Removal of Zn from recombinant BosR requires EDTA chelation under a denaturing condition. The Mn, Fe, Cu, and Zn levels in BosR were determined by ICP-SFMS and are shown as number of atoms per BosR dimer. BosR was analyzed as isolated (untreated) or after being mock treated or treated with 10 mM EDTA, either alone or in combination with urea (2 M) or SDS (0.1%). Data represent mean (±standard error of the mean [SEM]) of three readings of each sample. Values of treated samples were compared with those of the untreated sample using a two-way ANOVA, followed by Bonferroni posttest. Only *P* values of statistical significance are indicated: *, $P < 0.05$; ***, $P < 0.001$.

Next, we attempted to remove Zn from BosR by incubating the protein with 10 mM EDTA, either alone or in combination with 2 M urea or 0.1% SDS (Fig. 1). Only the EDTA-SDS treatment resulted in a significant reduction in the Zn level associated with BosR, reducing it from 1.72 to 0.06 atoms per dimer (Fig. 1). Notably, this result agrees with a previous report by others that recombinant BosR contained Zn, which could not be completely removed by EDTA treatment alone (44). Here, we show that this tightly associated Zn can be removed from BosR only under certain denaturing conditions, a property that resembles the S1 Zn first described in *B. subtilis* PerR (28), and we propose that this tightly bound Zn atom may be coordinated by the four cysteines conserved in BosR (Fig. S1 and S3).

The EDTA-SDS-treated BosR had an approximately 2-fold reduction in the DNA-binding activity compared to the mock-treated BosR (data not shown). While it is unexpected that BosR retained some activity after such a tightly associated Zn was stripped off, this result is consistent with a previous report by others in which recombinant BosR purified from inclusion bodies, presumably without any Zn, was shown to be capable of binding to DNA, and the addition of Zn increased the binding by only 2- to 3-fold (41). Mutagenesis studies targeting the cysteine residues of S1 would be required to determine whether this site indeed coordinates the Zn atom tightly associated with BosR and whether metal coordination at this site is required for BosR activity *in vivo*.

Other more modest (in comparison to the drastic reduction of Zn in the EDTA-SDS-treated sample) but nevertheless statistically significant increases in metal levels were detected in the mock-treated and EDTA-urea-treated samples (Fig. 1). Compared to the untreated sample, the mock-treated sample had an increase in the Zn level (from 1.72 to 2.62 atoms per dimer), indicating the presence of Zn in the buffer system or on the plastic filtration unit. The addition of 10 mM EDTA to the buffer system was able to eliminate this increase in Zn, as the EDTA-treated sample had no significant change in any metal level compared to the untreated sample. The EDTA-urea-treated sample had a slight increase in the Zn level (from 1.72 to 2.00 atoms per dimer) and a slight increase in the Cu level (from 0.06 to 0.30 atoms per dimer), compared to either the untreated or the EDTA-treated sample, suggesting that urea (which was used at a concentration of 2 M) may be a source of trace amounts of these metal ions. Overall, these modest increases in Zn and Cu levels are consistent with BosR being a metalloprotein and being capable of interacting with trace amounts of these metal ions present in the experimental system.

BosR has two additional metal-binding sites that can be occupied by Fe(II), Cu(II), or Zn(II) but not by Mn(II). To determine the capacity of BosR in binding additional metal ions, we either mock treated or incubated the protein (as isolated from

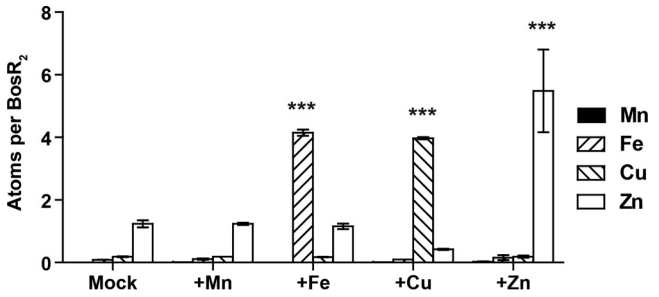

FIG 2 BosR has two additional metal-binding sites. Fe(II), Cu(II), and Zn(II), but not Mn(II), can be further incorporated into BosR to a level of approximately four atoms per dimer when metal ions were supplied at an 8-fold molar excess to BosR dimer. Data represent mean (±SEM) of the results from two independent samples. *P* values are derived from a two-way ANOVA, followed by Bonferroni posttest: ***, $P < 0.001$.

E. coli) with Mn(II), Fe(II), Cu(II), or Zn(II) at a molar ratio of eight metal ions per BosR dimer (see Materials and Methods for details). The mock-treated BosR had approximately 1.2 atoms of Zn and <0.2 atoms of Mn, Fe, or Cu per dimer (Fig. 2). Incubation with Mn(II) did not result in any significant change in the levels of any of these metals in BosR. Incubation with Fe(II), Cu(II), or Zn(II) resulted in an increase of approximately 4 atoms of the respective metal ion per BosR dimer. These data indicate that BosR has two additional metal-binding sites that can be occupied by Fe(II), Cu(II), or Zn(II) but not by Mn(II) under the same experimental conditions.

Interestingly, while incorporation of Fe(II) or Zn(II) did not affect the levels of other metal ions associated with BosR, incorporation of Cu(II) resulted in a significant reduction in the Zn level, from 1.2 to 0.4 atoms per dimer ($P = 0.02$, Student's *t* test). This suggests that Cu(II) coordination at these additional sites in BosR may result in conformational changes that destabilize the structural Zn(II) site.

Cu(II) and Zn(II) negatively regulate BosR DNA-binding activity. We used a fluorescence anisotropy (FA)-based DNA-binding assay developed in a previous study to determine the effects of Mn(II), Fe(II), Cu(II), and Zn(II) on BosR activity (see Materials and Methods for details). When the fluorescently labeled probe FP_{ospAB} (based on the BosR-binding site in the *ospAB* promoter) was incubated with increasing concentrations of BosR dimer, a dose-dependent binding was readily detected by measuring changes in FA (Fig. 3).

The addition of up to 10 μM Mn(II) or Fe(II) to the binding reactions had no effect on BosR binding to DNA (Fig. 3A and B). Further testing of these metal ions at higher concentrations, up to 100 μM for Mn(II) and up to 40 μM for Fe(II), also showed no effect (data not shown). Therefore, although Fe(II) and Mn(II) differ in their ability to occupy the regulatory sites of BosR, neither has an effect on the DNA-binding activity of BosR.

In contrast, the addition of up to 10 μM Cu(II) or Zn(II) to the binding reactions resulted in a dose-dependent inhibition of the DNA-binding activity of BosR (Fig. 3C and D). When these metal ions were tested at higher concentrations (20 μM and 40 μM), the binding curves were the same as that at 10 μM (data not shown), indicating that saturation of BosR (up to 1.5 μM dimer) was reached at 5 to 10 μM metal ion. The inhibitory effect of Cu(II) and Zn(II) on BosR activity appeared to be graded: the higher the ratio of metal ion to $BosR_2$, the stronger the inhibitory effect, with maximum inhibition achieved when the ratio reached approximately 4 (see data points in Fig. 3C and D).

Given that Fe(II) could bind to BosR but did not affect BosR activity, competition experiments were carried out to determine whether Fe(II) could dampen the inhibitory effect of Cu(II) or Zn(II). When Fe(II) was supplied at a 2-fold or 4-fold molar excess to Cu(II) or Zn(II), the DNA-binding activity of BosR was similarly inhibited as with Cu(II) or Zn(II) alone (Fig. S6). These results suggest that Cu(II) and Zn(II) have a higher affinity than Fe(II) for the regulatory metal-binding sites of BosR.

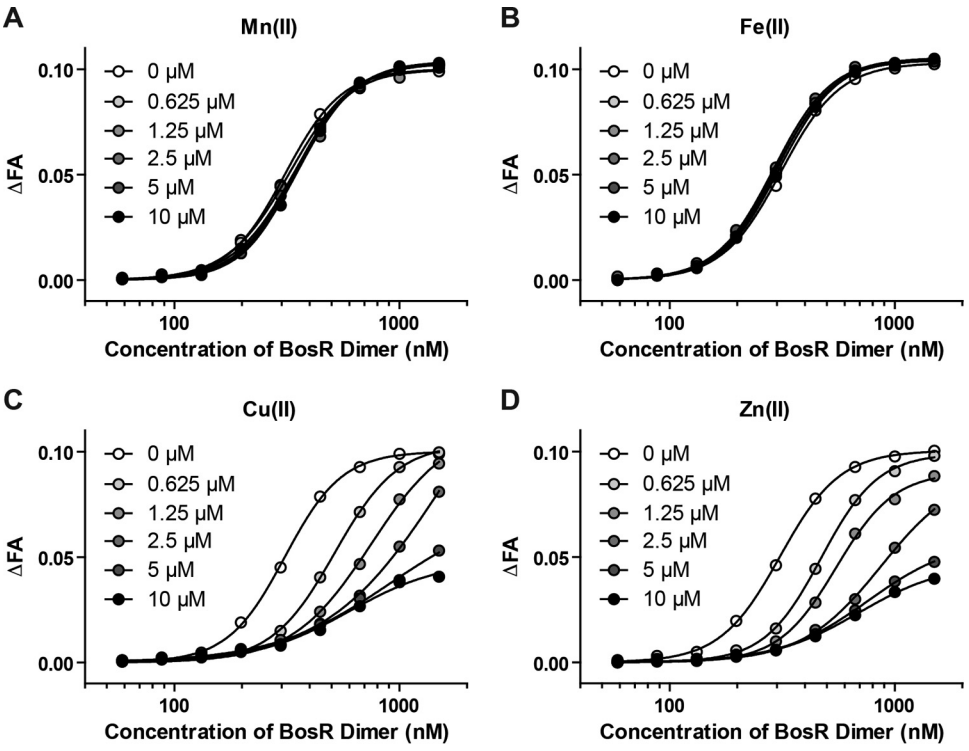

FIG 3 Cu(II) and Zn(II) inhibit BosR DNA-binding activity. The effect of Mn(II) (A), Fe(II) (B), Cu(II) (C), or Zn(II) (D) on BosR binding to a fluorescently labeled DNA probe was determined by measuring changes in fluorescence anisotropy (ΔFA). See Materials and Methods for details. The curves were fitted for one-site, specific binding with Hill slope using GraphPad Prism 6. R^2 was ≥0.99 for all curves.

Next, Cu(II) and Zn(II) were tested for their effect on a preformed $BosR_2$-DNA complex. The addition of Cu(II) and Zn(II) to binding reactions after the $BosR_2$-DNA complex had already formed resulted in a dose-dependent reduction in FA, indicating that these metal ions could trigger BosR dissociation from the fluorescently labeled DNA target (Fig. 4A). Here, again, the maximum inhibition was achieved at an approximate 4-fold molar ratio of Cu(II) to BosR dimer (Fig. 4A). The molar ratio of Zn(II) to BosR dimer at which the maximum inhibition was achieved, although varied among different preparations of BosR, was always slightly higher than the 4-fold molar excess required of Cu(II) (Fig. 4A and data not shown). This could be due to the different Zn levels associated with different preparations of BosR. One possibility is that the structural site has a higher affinity for Zn(II) than the regulatory sites. For BosR preparations with <2 atoms of Zn(II) per dimer, additional Zn(II) would be required to saturate the structural site before exerting an inhibitory effect at the regulatory sites.

Next, we tested whether EDTA could counter the inhibitory effects of Zn(II) and Cu(II). When EDTA was added to binding reaction mixtures to a final concentration of 1 mM, the inhibitory effect of Zn(II), but not that of Cu(II), was diminished (Fig. 4B). Additional experiments revealed that 10 μM EDTA was enough to counter the inhibitory effect of 10 μM Zn(II), whereas the inhibitory effect of Cu(II) was not affected by a 100-fold molar excess of EDTA (Fig. S7). We used their difference in susceptibilities to EDTA chelation after incorporation into BosR to determine whether Zn(II) or Cu(II) has a higher affinity for the regulatory sites, and the data indicated that Cu(II) had a higher affinity than Zn(II) for regulatory metal ion-binding sites of BosR when both were present at molar equivalent (Fig. S8).

Since Cu(II) is redox active and Zn(II) is redox inert, we next tested whether the reducing agent tris(2-carboxyethyl)phosphine (TCEP) could reverse the inhibitory effect of these metal ions on BosR DNA-binding activity. When TCEP was added to the binding reactions to a final concentration of 1 mM, the inhibitory effect of Cu(II) was abolished,

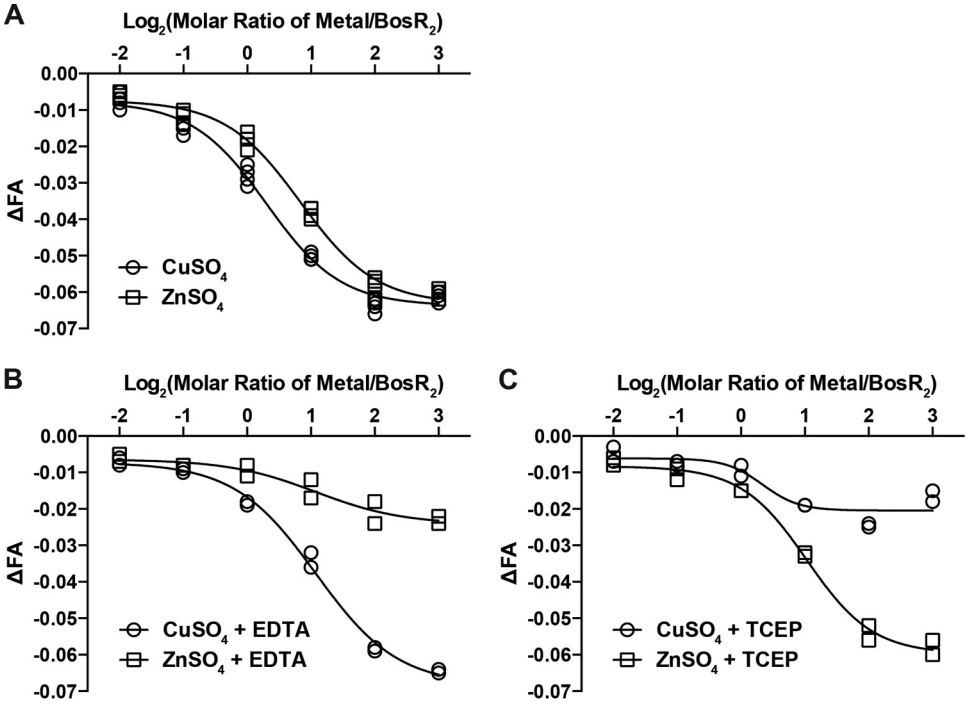

FIG 4 Cu(II) and Zn(II) trigger BosR dissociation from its DNA target. (A) When added to reactions after the formation of a $BosR_2$-DNA complex, Cu(II) and Zn(II) triggered $BosR_2$ dissociation from its DNA target, as evident in the dose-dependent reduction in FA. Four independent replicates were tested for each condition. (B) When EDTA was added to two of the replicates to a final concentration of 1 mM, it abolished the inhibitory effect of Zn(II) but not that of Cu(II). (C) When TCEP was added to the other two replicates to a final concentration of 1 mM, it abolished the inhibitory effect of Cu(II) but not that of Zn(II). The curves were fitted for dose response of inhibition with variable slope using GraphPad Prism 6. R^2 was $\geq$0.99 for all curves except those of $ZnSO_4$ plus EDTA and $CuSO_4$ plus TCEP, where the inhibitory effect of metal ions was significantly diminished.

whereas the inhibitory effect of Zn(II) was not affected (Fig. 4C). Similarly, when it was added to the binding reaction mixture containing Cu(II) prior to the addition of BosR, TCEP also abolished the inhibitory effect Cu(II) (data not shown). This selective countereffect of TCEP on Cu(II) but not Zn(II) is due to TCEP reduction of Cu(II) to Cu(I) (45).

Collectively, these data indicate that the two additional metal-binding sites in BosR play a regulatory role. Occupation of these sites by Cu(II) or Zn(II) results in an inhibition of BosR DNA-binding activity. Cu(II) has a higher affinity than Zn(II) for these regulatory sites, and inhibition of BosR by Cu(II) is responsive to redox regulation.

Increased Cu level in medium affects BosR-dependent differential expression of OspA/B and OspC in *B. burgdorferi*. To determine whether Cu affects BosR-dependent gene expression in *B. burgdorferi*, an infectious clone of the type strain B31 was cultivated in the Barbour-Stoenner-Kelly (BSK)-H complete medium (Sigma-Aldrich) supplemented with 0, 25, 50, or 100 μM $CuSO_4$. Although Cu is known to inhibit bacterial growth, an earlier study has established that at these concentrations, Cu has no significant impact on *B. burgdorferi* growth in the BSK-H complete medium (43). These cultures were grown at 37°C, because BosR-dependent induction of OspC and repression of OspA occur under conditions mimicking the mammalian host environment. As shown in a Coomassie blue-stained SDS-polyacrylamide gel (Fig. 5A), supplementation of the medium with Cu had a dose-dependent effect on the OspA/B and the OspC protein levels in *B. burgdorferi*: the higher the Cu level is in the medium, the higher the OspA/B level and the lower the OspC level. The changes in the OspA and OspC levels were further confirmed by immunoblot analyses (Fig. 5B).

To determine whether these changes in the OspA/B and the OspC protein levels are due to changes in their respective mRNA levels, *B. burgdorferi* was cultured at 37°C in the BSK-H complete medium, either not supplemented or supplemented with 100 μM $CuSO_4$, and three independent cultures were grown for each condition. Reverse

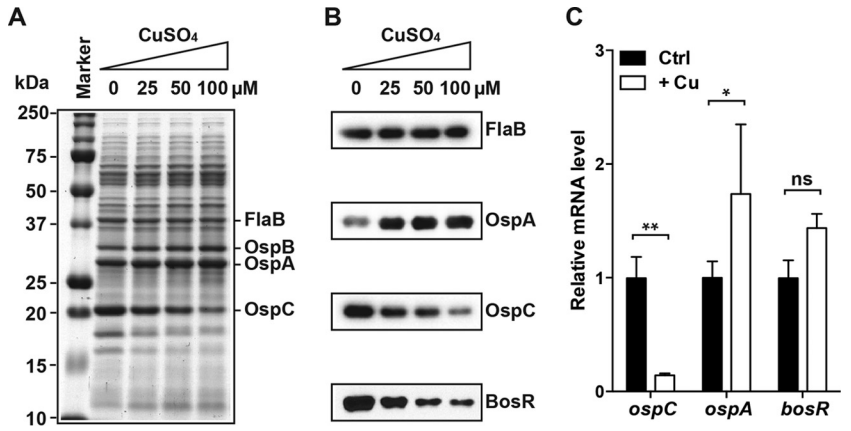

FIG 5 Cu level in the medium affects BosR-dependent gene expression in *B. burgdorferi*. (A) SDS-PAGE analysis of *B. burgdorferi* whole-cell lysates. A total of 10^7 cells were loaded on each lane. Spirochetes were grown in the BSK-H medium (Sigma-Aldrich) supplemented with 0, 25, 50, or 100 μM $CuSO_4$. (B) Immunoblot analyses of *B. burgdorferi* whole-cell lysates using antibodies specific to FlaB, OspA, OspC, or BosR. (C) Relative mRNA levels of *ospC*, *ospA*, and *bosR* of *B. burgdorferi* grown in the BSK-H medium either not supplemented (Ctrl) or supplemented with 100 μM $CuSO_4$ (+Cu) as determined by RT-qPCR analysis. Data represent means (plus standard deviations [SD]) of the results from three independent samples. The *ospC*, *ospA*, and *bosR* mRNA levels in each sample were first normalized against the *flaB* mRNA level. Then, the values of the treatment group were normalized against those of the control group. *P* values are derived from a two-way ANOVA, followed by Bonferroni posttest, and indicated as the following: ns, not significant; *, $P < 0.05$; **, $P < 0.01$.

transcription-quantitative PCR (RT-qPCR) analysis was performed to determine the *ospA* and *ospC* mRNA levels, which were then normalized against the *flaB* mRNA level. As shown in Fig. 5C, supplementation of the medium with Cu resulted in a significant reduction in the *ospC* mRNA level and a significant increase in the *ospA* mRNA level. Therefore, the changes in the OspA and OspC protein levels could be largely attributed to changes in their respective mRNA levels. These data agree with a large body of evidence indicating that differential expression of OspA and OspC occurs mostly at the transcriptional level (4, 5).

Based on the changes in the *ospA* and *ospC* mRNA levels, Cu supplementation of the growth medium apparently diminished BosR activity in *B. burgdorferi*. This reduction in the BosR activity correlated very well with a dose-dependent reduction in the BosR protein level as the Cu level increased (Fig. 5B) and therefore could not be directly attributed to Cu(II) negatively regulating BosR DNA-binding activity *per se*. Since the BosR mRNA level was comparable in *B. burgdorferi* grown with or without Cu supplementation (Fig. 5C), the negative effect of Cu on the BosR protein level likely happens at the posttranscriptional level. One possibility is that Cu(II) binding of BosR results in conformational changes that render the protein more susceptible to turnover or degradation *in vivo*. Several studies have indicated that BosR expression is regulated at both transcriptional and posttranscriptional levels (46–49).

BosR regulates Cu homeostasis in *B. burgdorferi*. To determine whether BosR is involved in regulating metal ion homeostasis in *B. burgdorferi*, we compared the cellular levels of Mn, Fe, Cu, and Zn among three isogenic strains that differ only in *bosR*, which were kindly provided by Michael Norgard (8). Spirochetes were cultivated at 25°C or 37°C to early stationary phase in BSK-H complete medium and then subjected to multielement analysis by ICP-SFMS (see Materials and Methods for details). There were both BosR-dependent (i.e., strain-dependent) and temperature-dependent variations in the cellular levels of these metals (Fig. 6).

Temperature had a significant effect on metal homeostasis in *B. burgdorferi* (Fig. 6). For all three strains analyzed here, spirochetes grown at 37°C had a significantly lower Mn level ($P < 0.001$), a significantly higher Cu level ($P < 0.01$), and a significantly lower Zn level ($P < 0.01$) than those grown at 25°C (two-way analysis of variance [ANOVA], followed by Bonferroni posttest). While there was a modest increase in the Fe level with

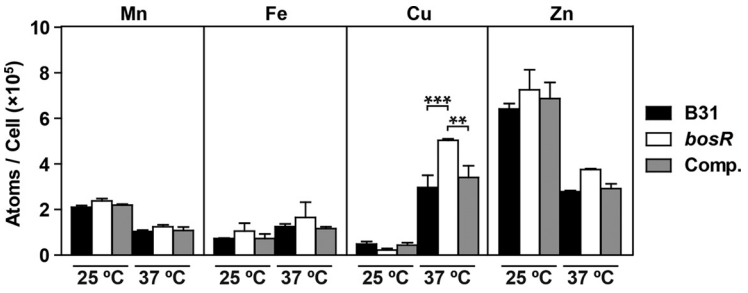

FIG 6 BosR regulates Cu homeostasis in *B. burgdorferi*. The Mn, Fe, Cu, and Zn levels in three isogenic B31 strains differing only in *bosR*, including the wild-type parental strain (WT), the *bosR* mutant (*bosR*), and the complemented *bosR* mutant (Comp.) were determined by ICP-SFMS. Spirochetes were cultivated microaerobically at 25°C or 37°C to early stationary phase in the BSK-H medium (Sigma-Aldrich). Data represent means (plus SEM) of the results from two independent samples. *P* values are derived from a two-way ANOVA, followed by Bonferroni posttest. For clarity, only *P* values for strain-dependent differences are indicated: **, $P < 0.01$; ***, $P < 0.001$; those for temperature-dependent differences are discussed only in the text.

the temperature shift from 25°C to 37°C, this difference was not statistically significant. Troxell and colleagues reported a similar temperature-dependent change in the Mn level in *B. burgdorferi*, a reduction at 37°C compared to 25°C (48). The molecular mechanisms underlying these changes as well as the biological significances of these changes remain unclear.

Of the four metal ions analyzed here, only the cellular level of Cu showed BosR-dependent variations (Fig. 6). Compared to its parental wild-type strain, the *bosR* mutant had a significantly higher level of Cu. Complementation of the mutant with a wild-type copy of *bosR* reduced the cellular Cu level to the wild-type level. Notably, these BosR-dependent differences were evident only at 37°C, which is consistent with BosR being expressed at 37°C but not at 25°C.

Overall, these data suggest that BosR is involved in regulating Cu homeostasis in *B. burgdorferi*. Since the presence of BosR leads to a reduction in the cellular Cu level, it is plausible to posit that BosR controls Cu homeostasis through the activation of Cu export and/or through the repression of import and/or storage. In addition, these data also point to factors other than BosR playing a role in maintaining Cu homeostasis in *B. burgdorferi*, because the drastic increase in the cellular Cu level at 37°C is independent of BosR.

Metalloregulation of BosR by Cu(II) may be an adaptation to the Cu-rich milieu in *B. burgdorferi*. The level of Cu detected in *B. burgdorferi*, $>10^5$ atoms of Cu per cell, is higher than the approximately 10^4 atoms per cell found in the model organism *E. coli* (50). For a direct comparison of transition metal ion levels between *B. burgdorferi* and *E. coli*, the *B. burgdorferi* type strain B31 and the *E. coli* K-12 strain TOP10 were both cultivated at 33°C in the BSK-H medium under microaerobic conditions. As expected, these two organisms differ considerably in growth rate, with *E. coli* reaching a saturation of 10^9 cells/ml in 16 h and *B. burgdorferi* reaching a saturation of 10^8 cells/ml in 10 days. Nevertheless, similar numbers of cells were harvested of both organisms (by using 10× volume of *B. burgdorferi* culture) for the ICP-SFMS analysis. Of these four metal ions analyzed (Fig. 7), only the Cu level differed significantly between *B. burgdorferi* and *E. coli* ($P < 0.001$, two-way ANOVA, followed by Bonferroni posttest). More specifically, the Cu level in *B. burgdorferi* (9.8×10^5 atoms per cell) is approximately 30-fold higher than that in *E. coli* (3.4×10^4 atoms per cell). There was also an approximately 30-fold difference in the Mn level, at 5.7×10^4 atoms per cell in *B. burgdorferi* compared to 1.5×10^3 atoms per cell in *E. coli*; however, this difference did not reach statistical significance.

Given that *E. coli* is routinely cultivated aerobically in LB, for further comparisons, the Mn, Fe, Cu, and Zn levels were determined for *E. coli* TOP10 cells grown under aerobic conditions (small culture volume with aeration) in either BSK-H medium or LB. Regard-

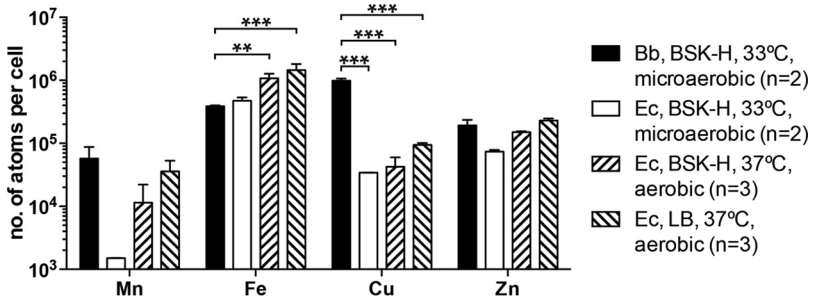

FIG 7 Cellular Cu level is much higher in *B. burgdorferi* (Bb) than in the model organism *E. coli* (Ec). The Mn, Fe, Cu, and Zn levels in the *B. burgdorferi* type strain B31 and the *E. coli* K-12 strain TOP10 were determined by ICP-SFMS. Both were cultivated microaerobically at 33°C to early stationary phase in the BSK-H medium (Sigma-Aldrich). In addition, TOP10 was cultivated aerobically at 37°C in the BSK-H medium and in LB. Data represent means (plus SD) of two or three biological replicates. *P* values are derived from a two-way ANOVA, followed by Bonferroni posttest. For clarity, only *P* values for comparisons between *B. burgdorferi* and *E. coli* are shown: **, $P < 0.01$; ***, $P < 0.001$.

less of the culture medium, *E. coli* cells grown aerobically had a much higher Fe level (1.1×10^6 and 1.4×10^6 atoms/cell for cells grown in BSK-H and LB, respectively) than *E. coli* (4.7×10^5 atoms/cell) or *B. burgdorferi* (3.9×10^5 atoms/cell) grown microaerobically in the BSK-H medium ($P < 0.05$, two-way ANOVA, followed by Bonferroni posttest) (Fig. 7). Although there were also increases in the Mn, Cu, and Zn levels of aerobically grown *E. coli* cells, these changes did not achieve statistical significance. The Cu level in *E. coli* grown aerobically (4.2×10^4 and 9.4×10^4 atoms per cell for cells grown in BSK-H and LB, respectively) is still significantly lower than the 9.8×10^5 atoms per cell level present in *B. burgdorferi* ($P < 0.001$, two-way ANOVA, followed by Bonferroni posttest) (Fig. 7).

It is worth noting that our measurements of these transition metal ion levels in *E. coli* agree strongly with data from other groups. The Fe level in *E. coli* ranges from 10^5 to 10^6 atoms per cell depending on growth conditions (51, 52), and a previous study determined the Fe level of *E. coli* grown aerobically in LB to be 1.2×10^6 atoms per cell (53), remarkably close to our measurement of 1.2×10^6 atoms per cell. The Cu level in *E. coli* was determined to be 3.6×10^4 to $\sim 7.8 \times 10^4$ atoms per cell in a previous study (54), which is again comparable to our measurement of 3.4×10^4 to $\sim 9.4 \times 10^4$ atoms per cell. The Zn and Mn levels in *E. coli* are estimated to be 10^5 and 10^4 atoms per cell (50), again consistent with our measurements.

In summary, a direct comparison with transition metal ion levels in the model organism *E. coli* has revealed that *B. burgdorferi* has an unusually high level of Cu. This leaves us to speculate that the prominent role of Cu(II) in the metalloregulation of BosR may be an adaptation to the Cu-rich milieu in the Lyme disease spirochete.

DISCUSSION

A common feature shared by the Fur family of transcriptional regulators is that their DNA-binding activity is often regulated by a divalent metal ion whose cellular homeostasis in turn is controlled by the same regulator (11, 25, 34). In this study, Cu(II) has emerged as the most prominent regulator of BosR DNA-binding activity *in vitro*, and it is also Cu homeostasis in *B. burgdorferi* that is the most significantly affected by a deficiency in BosR. This is the first time such a characteristic regulatory paradigm of the Fur family has been established for BosR, the sole Fur homologue in the Lyme disease spirochete, and to the best of our knowledge, BosR is the first Fur family member shown to be responsive to Cu(II).

As suggested by its name, BosR has long been implicated in regulating oxidative stress response in the Lyme disease spirochete (7, 41, 55, 56). Being a redox-active transition metal ion, Cu(II) offers a plausible mechanism for BosR to directly sense oxidative stress. BosR, like other Fur homologues, binds divalent metal ions. We did not detect any binding of Cu(I) to BosR or any effect of Cu(I) on the BosR activity (data not

shown). Moreover, TCEP, a reducing agent capable of reducing Cu(II) to Cu(I), could counter the inhibitory effect of Cu(II) on BosR activity. In *B. burgdorferi*, Cu(I) is largely sequestered by the *Borrelia* iron- and copper-binding protein A (BicA) (43). When *B. burgdorferi* was cultivated in the BSK-H medium, which contained 2 μM Cu (much of it being contributed by the 5% bovine serum albumin [BSA] and 6% rabbit serum in the medium), the cellular Cu level was approximately 750 μM in a wild-type strain and 30 μM in its isogenic *bicA*-deficient mutant (conversion from atoms/cell to molarity was based on an estimated volume of 10^{-9} μl for an average spirochete of $\sim$300 nm in diameter and 15 μm in length) (43). Since Cu sequestered by the metallothionein domain of BicA is in the cuprous form, it would have to be oxidized to exert any effect on BosR. It has been shown that BicA-bound Cu(I) is reactive with hydrogen peroxide (43). Therefore, it is possible for BosR to sense peroxide stress through binding of Cu(II), a product of the Fenton-like reaction between Cu(I) and hydrogen peroxide. A commonality between this proposed model for peroxide sensing by *B. burgdorferi* BosR and the mechanism of peroxide by *B. subtilis* PerR appears to be the employment of a redox-active metal ion at the regulatory site(s), Fe(II) for PerR and Cu(II) for BosR.

Not only is BosR the first of the Fur family shown to be responsive to Cu, many other features of BosR also set it apart from other Fur family members. The DNA-binding activity of BosR was inhibited by metal ion coordination by either Zn(II) or Cu(II) at the regulatory sites. In contrast, most other Fur family members, including *B. subtilis* PerR, require metal ion coordination at the regulatory site(s) (S2 and/or S3) to become active in DNA binding. However, in light of BosR not having either the S2 or the S3 site, this mechanistic difference perhaps should not come as a surprise. The compositions of the two regulatory metal ion coordination sites identified in BosR in this study remain to be defined by crystallography but are expected to be different from those of S2 and S3.

While the direct effect of a specific transition metal ion on the BosR DNA-binding activity can be assessed in a straightforward manner using *in vitro* biochemical analyses, it is much more difficult to ascertain/decipher the *in vivo* cellular effect(s) of a specific transition metal ion on BosR activity. Given the prominent role of Cu(II) in negatively regulating the BosR activity *in vitro*, we attempted to examine the effect of Cu on the BosR activity in *B. burgdorferi*. Supplementation of the growth medium with Cu indeed diminished BosR activity at the cellular level, which is reflected in an increase in OspA expression and a reduction in OspC expression. While this result is in agreement with Cu being a negative regulator of BosR activity, further analysis showed that the negative effect could be explained by a reduction in the BosR protein level, which led us to hypothesize that Cu(II)-loaded BosR may be more susceptible to degradation or turnover *in vivo*. Cu(II) could compete with Zn(II) for the same structural site, as indicated by a reduction of Zn(II) in Cu(II)-loaded BosR (Fig. 2), which may interfere with BosR dimerization and render it less stable. Since Fe(II) had no regulatory effect on BosR activity *in vitro*, we did not further assess the *in vivo* effect(s) of Fe in this study. As for Mn and Zn, it has been reported that Mn represses whereas Zn activates BosR-dependent OspC expression (48). Therefore, the cellular effects of Mn (negative) and Zn (positive) on BosR activity do not correlate with the direct effects of Mn(II) (neutral) and Zn(II) (negative) on the DNA-binding activity of BosR.

Transition metal ions can affect cellular functions in many different ways. Here, we discuss just two alternative explanations for the repressive effect of Mn on the BosR activity in *B. burgdorferi* that do not rely on a direct interaction between Mn(II) and BosR. Various transition metal ions in *B. burgdorferi* are intricately connected with each other in homeostasis, and disturbance in one often leads to changes in others (43). For example, a deficiency in the manganese-specific metal transporter BmtA leads to a significant reduction in Mn, but this change is accompanied by a significant reduction in Cu and significant increases in Fe and Zn (43, 57). Therefore, the enhanced BosR activity observed of the *bmtA* mutant could be attributed more directly to the reduced level of Cu instead of the reduced level of Mn. Another way by which Mn could impact the BosR activity in *B. burgdorferi* is through the superoxide dismutase SodA. Despite an earlier report to the contrary (58), two recent studies have shown that *B. burgdorferi*

SodA utilizes Mn(II) instead of Fe(II) as a cofactor, and there is a positive correlation between the Mn level and SodA enzymatic activity (59, 60). Thus, a higher Mn level could lead to greater production of hydrogen peroxide, which in turn could drive the redox state of Cu from Cu(I) toward Cu(II) and inhibit BosR activity. These alternative explanations highlight the difficulty in deciphering the cellular effects of specific metal ions.

During the transition from the tick to the mammal, *B. burgdorferi* senses environmental signals, such as changes in temperature, pH, and nutrients, through many regulatory pathways (4, 5). Copper and zinc levels in serum are estimated to be in the range of 10 to 25 μM, but their levels in the tick midgut are expected to be higher, because the hard-bodied *Ixodes* ticks are known to concentrate their blood meal during feeding. Existing evidence suggests that regulation of BosR expression (at both transcriptional and posttranscriptional levels) could play a much more important role than metalloregulation of BosR activity. The focus of this study, metalloregulation of BosR, represents only one facet of a very complex regulatory network in *B. burgdorferi*, and its role in the spirochete's natural life cycle remains to be explored. Such an investigation would require more in-depth understanding of the regulatory sites of BosR and construction and characterization of *B. burgdorferi* strains expressing mutant BosR defective in metal ion sensing.

MATERIALS AND METHODS

Strains, media, and other reagents. *Escherichia coli* strain M15 (Qiagen) was used as the host cell for overexpression of BosR and was grown at 37°C in Luria-Bertani (LB) medium. *Borrelia burgdorferi* type strain B31 and its isogenic *bosR* mutant and the complemented *bosR* mutant were kindly provided by Michael Norgard at the University of Texas Southwestern Medical Center (8). Spirochetes were cultivated at 25°C, 33°C, and 37°C in BSK-H complete medium (Sigma-Aldrich) to early stationary phase under microaerobic conditions by growing cultures in closed tubes with a small void space at the top (e.g., 45 ml of culture in a closed 50-ml conical tube). When indicated, $CuSO_4$ was added to the BSK-H medium to a specified concentration prior to cultivation. All chemical reagents, unless otherwise noted, were purchased from Sigma-Aldrich and were of either BioReagent or ReagentPlus grade.

Expression and purification of recombinant tag-free BosR. Expression and purification of recombinant BosR were performed as previously described (6). Briefly, BosR was overexpressed in *E. coli* as a His_6-tagged protein and then affinity purified on the HisPur cobalt resin (Thermo Scientific). The amino-terminal His_6 tag was subsequently cleaved off by dipeptidyl aminopeptidase I (Qiagen). Any remaining tagged protein (due to incomplete digestion) was removed by passing the sample through the HisPur cobalt resin the second time (see Fig. S4 in the supplemental material). Purified protein was stored in small aliquots at −80°C until use. Protein concentration was determined by the Bradford assay (Bio-Rad), in which BSA solutions with known concentrations were used as standards, and by absorbance at a 280 nm wavelength, in which the extinction coefficient for the tag-free BosR was calculated as 15,930 $M^{-1} \cdot cm^{-1}$ or 0.788 $(g/liter)^{-1} \cdot cm^{-1}$ using the ExPASy ProtParam tool. The results from these two methods were comparable (Table S1). The molecular mass of purified tag-free BosR was estimated to be 37.6 kDa by size-exclusion chromatography using a Superdex 75 (10/300) column, which is consistent with a dimer (Fig. S5).

Metal removal and metal incorporation into recombinant BosR. For metal removal, BosR (125 μM) was incubated in phosphate-buffered saline (PBS; Life Technologies) at room temperature for 2 h with 10 mM EDTA, either alone or in combination with 2 M urea (Teknova) or 0.1% SDS. The samples were then washed with PBS and filtered three times using centrifugal filter units (Millipore) with a 10-kDa molecular mass cutoff. For metal incorporation, BosR (20 μM) was incubated at room temperature for 10 min with 4-fold molar excess of $MnSO_4$, $Fe(NH_4)_2(SO_4)_2$, $CuSO_4$, or $ZnSO_4$ in a buffer containing 10 mM Tris (pH 7.5) and 50 mM KCl. After incubation, samples were washed three times with the Tris-KCl buffer and filtered using centrifugal filter units with a 10-kDa molecular mass cutoff (Millipore).

Metal analysis. Metal levels were determined by inductively coupled plasma-sector field mass spectrometry (ICP-SFMS) using a Thermo Finnigan Element 2 instrument at the Trace Element Research Laboratory of The Ohio State University, as previously described (43). Briefly, samples (bacteria or protein) were digested with nitric acid, and indium (In) was added as an internal standard to each sample to a final concentration of 10 ppb. Dilutions (1 ppb, 10 ppb, 50 ppb, and 200 ppb) of a certified standard (containing 48 elements, including Mn, Fe, Cu, Zn, and In) were used to generate linear calibration curves.

Fluorescence anisotropy. As described in a previous study (6), the 6-carboxyfluorescein (FAM)-labeled probe (10 nM) was incubated with BosR (at concentrations ranging from 30 to 2,000 nM dimer) for 5 min at room temperature in 20-μl reaction mixtures containing 10 mM Tris (pH 7.5) and 100 mM KCl, and binding of BosR to the probe was monitored by measuring changes in fluorescence anisotropy (ΔFA; λ excitation [λ_{ex}] = 470 nM; λ emission [λ_{em}] = 520 nM) using a Tecan Infinite M1000Pro instrument equipped with the iControl software version 1.9 or using a BioTek Synergy H1 instrument equipped with the Gen5 software.

In a previous study, we had shown that BosR bound to 6-FAM-labeled probes in a sequence-specific manner: it had a much higher affinity for probes based on the BosR-binding sites identified in the *ospAB* promoter (FP_{ospAB}) and the *ospD* promoter (FP_{ospD}) than for probes of a random sequence of As and Ts (FP_{RndAT}) or a random sequence of As, Ts, Gs, and Cs (FP_{Rnd}) (6). To further demonstrate the sequence specificity of BosR binding to FP_{ospAB}, a competition experiment was performed in which BosR was preincubated with unlabeled probes before binding to FP_{ospAB}. Preincubation of BosR with P_{ospAB}, the unlabeled probe of the same sequence as FP_{ospAB}, inhibited BosR binding to FP_{ospAB} in a dose-dependent manner, whereas preincubation with P_{RndAT} and P_{Rnd} had a moderate and no inhibitory effect, respectively (Fig. S9).

Several reagents, including EDTA, a strong chelator of metal ions, TCEP, a potent reducing agent (61), and dithiothreitol (DTT), a potent reducing agent that is also a strong chelator of metal ions (62), were tested for their effect on BosR binding to FP_{ospAB}. The reducing agent TCEP (1 mM) had no effect, whereas DTT (1 mM) and EDTA (10 μM) had similar slight stimulatory effects (Fig. S10). These data are consistent with the presence of an inhibitory factor(s) in the binding reactions, which can be chelated by DTT and EDTA.

To test the effect of metal ions on BosR binding to FP_{ospAB}, $MnSO_4$, $Fe(NH_4)_2(SO_4)_2$, $CuSO_4$, or $ZnSO_4$ was added to the binding reactions to a final concentration of 0, 0.625, 1.25, 2.5, 5, or 10 μM. When indicated, EDTA was added to binding reactions to a specified concentration either before or after BosR was incubated with the probe in the presence of Zn(II) and/or Cu(II). To minimize Fe(II) oxidation, the 100 mM stock solution of $Fe(NH_4)_2(SO_4)_2$ was freshly prepared in 0.1% HCl containing 1 mM sodium dithionite, and *N*-acetyl cysteine was added to the binding reactions to a final concentration of 1 mM. Under these conditions, oxidation was not detected when Fe(II) was tested at concentrations up to 10 μM.

To test whether Zn(II) and Cu(II) can trigger dissociation of BosR from FP_{ospAB}, the probe (10 nM) was first incubated with BosR (2 μM dimer) for 5 min, and then $CuSO_4$ or $ZnSO_4$ was added to the reactions to a final concentration of 0, 0.25, 0.5, 1, 2, 4, 8, or 16 μM. Four replicates were tested for each condition. To further determine whether EDTA or TCEP could reverse the inhibitory effects of these metal ions, these reagents were added separately to two sets of the replicate reactions to a final concentration of 1 mM. Changes in fluorescence anisotropy were recorded before and after the addition of metal ions and again after the addition of EDTA or TCEP.

SDS-PAGE and immunoblot analysis. Bacterial pellets were suspended in the Laemmli buffer (63) to 2×10^6 spirochetes/μl and incubated at 100°C for 10 min. Samples (5 μl/lane) were subjected to SDS-PAGE on gels containing 12% polyacrylamide in the resolving layer. Protein bands were visualized by staining with Coomassie brilliant blue or transferred to nitrocellulose membranes for blotting with specific antibodies. The anti-BosR, anti-OspA, and anti-OspC antisera were separately raised in mice using the respective recombinant proteins. The anti-BosR antiserum was used at a 1:2,000 dilution, and the anti-OspA and anti-OspC antisera were used at a 1:5,000 dilution. A monoclonal antibody against FlaB (H9724) described previously (64) was used at a 1:100 dilution. For the secondary antibody, a goat anti-mouse IgG-horseradish peroxidase conjugate was purchased from Kirkegaard & Perry Laboratories and used at a 1:10,000 dilution. Signals were developed using the SuperSignal West Pico chemiluminescent substrate (Thermo Scientific) and captured on X-ray films or a digital imager.

RNA extraction and RT-qPCR analysis. Total RNA was extracted from *in vitro*-grown spirochetes using the TRIzol reagent (Life Technologies). After digestion with RNase-free DNase (Roche) to remove DNA contamination, RNA was further purified on the RNeasy minispin columns (Qiagen). For RT-qPCR analysis, RNA was first converted into first-strand cDNA using random hexamers and the SuperScript III reverse transcriptase (Life Technologies), and then the gene copy numbers in the cDNA were determined using the SYBR green real-time PCR master mix (Life Technologies). Gene-specific primers for *B. burgdorferi ospA*, *ospC*, *bosR*, and *flaB* used here were the same as those described previously (6). All procedures were carried out according to the manufacturers' recommendations.

Statistical analysis. All statistical and graphic analyses were performed using the software GraphPad Prism 6 for Mac OS X (version 6.0e). All reported *P* values are 2-tailed. *P* values of <0.05 are considered statistically significant. The specific statistical test for each *P* value is indicated in the text.

SUPPLEMENTAL MATERIAL

Supplemental material for this article may be found at https://doi.org/10.1128/JB.00276-17.

SUPPLEMENTAL FILE 1, PDF file, 2.0 MB.

ACKNOWLEDGMENTS

We thank Michael Norgard for providing strains, Jeremy Whitson, Mary Carter, and Andrea Koenigsberg for technical support, and Frank Gherardini, John Leong, and Meghan Ramsey for helpful discussions.

This study was supported by grant 1R01AI103173 from the National Institutes of Health (to X.L.). The work in the Heldwein lab was supported by the NIH grants 1R01GM111795 and 1R21AI107171, the Investigators in the Pathogenesis of Infectious Disease from Burroughs Wellcome Fund, and a Faculty Scholar grant from the Howard Hughes Medical Institute.

REFERENCES

1. Steere AC. 2001. Lyme disease. N Engl J Med 345:115–125. https://doi.org/10.1056/NEJM200107123450207.
2. Stanek G, Wormser GP, Gray J, Strle F. 2012. Lyme borreliosis. Lancet 379:461–473. https://doi.org/10.1016/S0140-6736(11)60103-7.
3. Piesman J, Gern L. 2004. Lyme borreliosis in Europe and North America. Parasitology 129(Suppl):S191–220.
4. Samuels DS. 2011. Gene regulation in *Borrelia burgdorferi*. Annu Rev Microbiol 65:479–499. https://doi.org/10.1146/annurev.micro.112408.134040.
5. Radolf JD, Caimano MJ, Stevenson B, Hu LT. 2012. Of ticks, mice and men: understanding the dual-host lifestyle of Lyme disease spirochaetes. Nat Rev Microbiol 10:87–99.
6. Wang P, Dadhwal P, Cheng Z, Zianni MR, Rikihisa Y, Liang FT, Li X. 2013. Borrelia burgdorferi oxidative stress regulator BosR directly represses lipoproteins primarily expressed in the tick during mammalian infection. Mol Microbiol 89:1140–1153. https://doi.org/10.1111/mmi.12337.
7. Hyde JA, Shaw DK, Smith R, III, Trzeciakowski JP, Skare JT. 2009. The BosR regulatory protein of *Borrelia burgdorferi* interfaces with the RpoS regulatory pathway and modulates both the oxidative stress response and pathogenic properties of the Lyme disease spirochete. Mol Microbiol 74:1344–1355. https://doi.org/10.1111/j.1365-2958.2009.06951.x.
8. Ouyang Z, Kumar M, Kariu T, Haq S, Goldberg M, Pal U, Norgard MV. 2009. BosR (BB0647) governs virulence expression in *Borrelia burgdorferi*. Mol Microbiol 74:1331–1343. https://doi.org/10.1111/j.1365-2958.2009.06945.x.
9. Hantke K. 1981. Regulation of ferric iron transport in *Escherichia coli* K-12: isolation of a constitutive mutant. Mol Gen Genet 182:288–292. https://doi.org/10.1007/BF00269672.
10. Bagg A, Neilands JB. 1987. Ferric uptake regulation protein acts as a repressor, employing iron (II) as a cofactor to bind the operator of an iron transport operon in *Escherichia coli*. Biochemistry 26:5471–5477. https://doi.org/10.1021/bi00391a039.
11. Lee JW, Helmann JD. 2007. Functional specialization within the Fur family of metalloregulators. Biometals 20:485–499. https://doi.org/10.1007/s10534-006-9070-7.
12. Ahn BE, Cha J, Lee EJ, Han AR, Thompson CJ, Roe JH. 2006. Nur, a nickel-responsive regulator of the Fur family, regulates superoxide dismutases and nickel transport in Streptomyces coelicolor. Mol Microbiol 59:1848–1858. https://doi.org/10.1111/j.1365-2958.2006.05065.x.
13. Díaz-Mireles E, Wexler M, Sawers G, Bellini D, Todd JD, Johnston AW. 2004. The Fur-like protein Mur of Rhizobium leguminosarum is a Mn^{2+}-responsive transcriptional regulator. Microbiology 150:1447–1456. https://doi.org/10.1099/mic.0.26961-0.
14. Gaballa A, Helmann JD. 1998. Identification of a zinc-specific metalloregulatory protein, Zur, controlling zinc transport operons in *Bacillus subtilis*. J Bacteriol 180:5815–5821.
15. Patzer SI, Hantke K. 1998. The ZnuABC high-affinity zinc uptake system and its regulator Zur in *Escherichia coli*. Mol Microbiol 28:1199–1210. https://doi.org/10.1046/j.1365-2958.1998.00883.x.
16. Lee JW, Helmann JD. 2006. The PerR transcription factor senses H_2O_2 by metal-catalysed histidine oxidation. Nature 440:363–367. https://doi.org/10.1038/nature04537.
17. Qi Z, Hamza I, O'Brian MR. 1999. Heme is an effector molecule for iron-dependent degradation of the bacterial iron response regulator (Irr) protein. Proc Natl Acad Sci U S A 96:13056–13061. https://doi.org/10.1073/pnas.96.23.13056.
18. Troxell B, Hassan HM. 2013. Transcriptional regulation by ferric uptake regulator (Fur) in pathogenic bacteria. Front Cell Infect Microbiol 3:59. https://doi.org/10.3389/fmicb.2013.00059.
19. Hantke K. 2001. Iron and metal regulation in bacteria. Curr Opin Microbiol 4:172–177. https://doi.org/10.1016/S1369-5274(00)00184-3.
20. Carpenter BM, Whitmire JM, Merrell DS. 2009. This is not your mother's repressor: the complex role of fur in pathogenesis. Infect Immun 77:2590–2601. https://doi.org/10.1128/IAI.00116-09.
21. Davies BW, Bogard RW, Mekalanos JJ. 2011. Mapping the regulon of *Vibrio cholerae* ferric uptake regulator expands its known network of gene regulation. Proc Natl Acad Sci U S A 108:12467–12472. https://doi.org/10.1073/pnas.1107894108.
22. Butcher J, Sarvan S, Brunzelle JS, Couture JF, Stintzi A. 2012. Structure and regulon of *Campylobacter jejuni* ferric uptake regulator Fur define apo-Fur regulation. Proc Natl Acad Sci U S A 109:10047–10052. https://doi.org/10.1073/pnas.1118321109.
23. Pich OQ, Carpenter BM, Gilbreath JJ, Merrell DS. 2012. Detailed analysis of Helicobacter pylori Fur-regulated promoters reveals a Fur box core sequence and novel Fur-regulated genes. Mol Microbiol 84:921–941. https://doi.org/10.1111/j.1365-2958.2012.08066.x.
24. Seo SW, Kim D, Latif H, O'Brien EJ, Szubin R, Palsson BO. 2014. Deciphering Fur transcriptional regulatory network highlights its complex role beyond iron metabolism in *Escherichia coli*. Nat Commun 5:4910. https://doi.org/10.1038/ncomms5910.
25. An YJ, Ahn BE, Han AR, Kim HM, Chung KM, Shin JH, Cho YB, Roe JH, Cha SS. 2009. Structural basis for the specialization of Nur, a nickel-specific Fur homolog, in metal sensing and DNA recognition. Nucleic Acids Res 37:3442–3451. https://doi.org/10.1093/nar/gkp198.
26. Pohl E, Haller JC, Mijovilovich A, Meyer-Klaucke W, Garman E, Vasil ML. 2003. Architecture of a protein central to iron homeostasis: crystal structure and spectroscopic analysis of the ferric uptake regulator. Mol Microbiol 47:903–915. https://doi.org/10.1046/j.1365-2958.2003.03337.x.
27. Pecqueur L, D'Autreaux B, Dupuy J, Nicolet Y, Jacquamet L, Brutscher B, Michaud-Soret I, Bersch B. 2006. Structural changes of Escherichia coli ferric uptake regulator during metal-dependent dimerization and activation explored by NMR and X-ray crystallography. J Biol Chem 281:21286–21295. https://doi.org/10.1074/jbc.M601278200.
28. Traoré DA, El Ghazouani A, Ilango S, Dupuy J, Jacquamet L, Ferrer JL, Caux-Thang C, Duarte V, Latour JM. 2006. Crystal structure of the apo-PerR-Zn protein from *Bacillus subtilis*. Mol Microbiol 61:1211–1219. https://doi.org/10.1111/j.1365-2958.2006.05313.x.
29. Lucarelli D, Russo S, Garman E, Milano A, Meyer-Klaucke W, Pohl E. 2007. Crystal structure and function of the zinc uptake regulator FurB from *Mycobacterium tuberculosis*. J Biol Chem 282:9914–9922. https://doi.org/10.1074/jbc.M609974200.
30. Jacquamet L, Traore DA, Ferrer JL, Proux O, Testemale D, Hazemann JL, Nazarenko E, El Ghazouani A, Caux-Thang C, Duarte V, Latour JM. 2009. Structural characterization of the active form of PerR: insights into the metal-induced activation of PerR and Fur proteins for DNA binding. Mol Microbiol 73:20–31. https://doi.org/10.1111/j.1365-2958.2009.06753.x.
31. Sheikh MA, Taylor GL. 2009. Crystal structure of the *Vibrio cholerae* ferric uptake regulator (Fur) reveals insights into metal co-ordination. Mol Microbiol 72:1208–1220. https://doi.org/10.1111/j.1365-2958.2009.06718.x.
32. Traoré DA, El Ghazouani A, Jacquamet L, Borel F, Ferrer JL, Lascoux D, Ravanat JL, Jaquinod M, Blondin G, Caux-Thang C, Duarte V, Latour JM. 2009. Structural and functional characterization of 2-oxo-histidine in oxidized PerR protein. Nat Chem Biol 5:53–59. https://doi.org/10.1038/nchembio.133.
33. Dian C, Vitale S, Leonard GA, Bahlawane C, Fauquant C, Leduc D, Muller C, de Reuse H, Michaud-Soret I, Terradot L. 2011. The structure of the *Helicobacter pylori* ferric uptake regulator Fur reveals three functional metal binding sites. Mol Microbiol 79:1260–1275. https://doi.org/10.1111/j.1365-2958.2010.07517.x.
34. Shin JH, Jung HJ, An YJ, Cho YB, Cha SS, Roe JH. 2011. Graded expression of zinc-responsive genes through two regulatory zinc-binding sites in Zur. Proc Natl Acad Sci U S A 108:5045–5050. https://doi.org/10.1073/pnas.1017744108.
35. Makthal N, Rastegari S, Sanson M, Ma Z, Olsen RJ, Helmann JD, Musser JM, Kumaraswami M. 2013. Crystal structure of peroxide stress regulator from Streptococcus pyogenes provides functional insights into the mechanism of oxidative stress sensing. J Biol Chem 288:18311–18324. https://doi.org/10.1074/jbc.M113.456590.
36. Gilston BA, Wang S, Marcus MD, Canalizo-Hernandez MA, Swindell EP, Xue Y, Mondragon A, O'Halloran TV. 2014. Structural and mechanistic basis of zinc regulation across the *E. coli* Zur regulon. PLoS Biol 12:e1001987. https://doi.org/10.1371/journal.pbio.1001987.
37. Lin CS, Chao SY, Hammel M, Nix JC, Tseng HL, Tsou CC, Fei CH, Chiou HS, Jeng US, Lin YS, Chuang WJ, Wu JJ, Wang S. 2014. Distinct structural features of the peroxide response regulator from group A *Streptococcus* drive DNA binding. PLoS One 9:e89027. https://doi.org/10.1371/journal.pone.0089027.
38. Deng Z, Wang Q, Liu Z, Zhang M, Machado AC, Chiu TP, Feng C, Zhang Q, Yu L, Qi L, Zheng J, Wang X, Huo X, Qi X, Li X, Wu W, Rohs R, Li Y, Chen Z. 2015. Mechanistic insights into metal ion activation and operator

recognition by the ferric uptake regulator. Nat Commun 6:7642. https://doi.org/10.1038/ncomms8642.
39. Fraser CM, Casjens S, Huang WM, Sutton GG, Clayton R, Lathigra R, White O, Ketchum KA, Dodson R, Hickey EK, Gwinn M, Dougherty B, Tomb JF, Fleischmann RD, Richardson D, Peterson J, Kerlavage AR, Quackenbush J, Salzberg S, Hanson M, van Vugt R, Palmer N, Adams MD, Gocayne J, Venter JC. 1997. Genomic sequence of a Lyme disease spirochaete, *Borrelia burgdorferi*. Nature 390:580–586. https://doi.org/10.1038/37551.
40. Samuels DS, Radolf JD. 2009. Who is the BosR around here anyway? Mol Microbiol 74:1295–1299. https://doi.org/10.1111/j.1365-2958.2009.06971.x.
41. Boylan JA, Posey JE, Gherardini FC. 2003. *Borrelia* oxidative stress response regulator, BosR: a distinctive Zn-dependent transcriptional activator. Proc Natl Acad Sci U S A 100:11684–11689. https://doi.org/10.1073/pnas.2032956100.
42. Katona LI, Tokarz R, Kuhlow CJ, Benach J, Benach JL. 2004. The Fur homologue in *Borrelia burgdorferi*. J Bacteriol 186:6443–6456. https://doi.org/10.1128/JB.186.19.6443-6456.2004.
43. Wang P, Lutton A, Olesik J, Vali H, Li X. 2012. A novel iron- and copper-binding protein in the Lyme disease spirochaete. Mol Microbiol 86:1441–1451. https://doi.org/10.1111/mmi.12068.
44. Ouyang Z, Deka RK, Norgard MV. 2011. BosR (BB0647) controls the RpoN-RpoS regulatory pathway and virulence expression in *Borrelia burgdorferi* by a novel DNA-binding mechanism. PLoS Pathog 7:e1001272. https://doi.org/10.1371/journal.ppat.1001272.
45. Krezel A, Latajka R, Bujacz GD, Bal W. 2003. Coordination properties of tris(2-carboxyethyl)phosphine, a newly introduced thiol reductant, and its oxide. Inorg Chem 42:1994–2003. https://doi.org/10.1021/ic025969y.
46. Hyde JA, Trzeciakowski JP, Skare JT. 2007. Borrelia burgdorferi alters its gene expression and antigenic profile in response to CO_2 levels. J Bacteriol 189:437–445. https://doi.org/10.1128/JB.01109-06.
47. Sze CW, Smith A, Choi YH, Yang X, Pal U, Yu A, Li C. 2013. Study of the response regulator Rrp1 reveals its regulatory role in chitobiose utilization and virulence of Borrelia burgdorferi. Infect Immun 81:1775–1787. https://doi.org/10.1128/IAI.00050-13.
48. Troxell B, Ye M, Yang Y, Carrasco SE, Lou Y, Yang XF. 2013. Manganese and zinc regulate virulence determinants in Borrelia burgdorferi. Infect Immun 81:2743–2752. https://doi.org/10.1128/IAI.00507-13.
49. He M, Zhang JJ, Ye M, Lou Y, Yang XF. 2014. Cyclic di-GMP receptor PlzA controls virulence gene expression through RpoS in Borrelia burgdorferi. Infect Immun 82:445–452. https://doi.org/10.1128/IAI.01238-13.
50. Finney LA, O'Halloran TV. 2003. Transition metal speciation in the cell: insights from the chemistry of metal ion receptors. Science 300:931–936. https://doi.org/10.1126/science.1085049.
51. Abdul-Tehrani H, Hudson AJ, Chang YS, Timms AR, Hawkins C, Williams JM, Harrison PM, Guest JR, Andrews SC. 1999. Ferritin mutants of *Escherichia coli* are iron deficient and growth impaired, and *fur* mutants are iron deficient. J Bacteriol 181:1415–1428.
52. Andrews SC, Robinson AK, Rodriguez-Quinones F. 2003. Bacterial iron homeostasis. FEMS Microbiol Rev 27:215–237. https://doi.org/10.1016/S0168-6445(03)00055-X.
53. Nunoshiba T, Obata F, Boss AC, Oikawa S, Mori T, Kawanishi S, Yamamoto K. 1999. Role of iron and superoxide for generation of hydroxyl radical, oxidative DNA lesions, and mutagenesis in Escherichia coli. J Biol Chem 274:34832–34837. https://doi.org/10.1074/jbc.274.49.34832.
54. Fung DK, Lau WY, Chan WT, Yan A. 2013. Copper efflux is induced during anaerobic amino acid limitation in Escherichia coli to protect iron-sulfur cluster enzymes and biogenesis. J Bacteriol 195:4556–4568. https://doi.org/10.1128/JB.00543-13.
55. Seshu J, Boylan JA, Hyde JA, Swingle KL, Gherardini FC, Skare JT. 2004. A conservative amino acid change alters the function of BosR, the redox regulator of Borrelia burgdorferi. Mol Microbiol 54:1352–1363. https://doi.org/10.1111/j.1365-2958.2004.04352.x.
56. Hyde JA, Seshu J, Skare JT. 2006. Transcriptional profiling of *Borrelia burgdorferi* containing a unique *bosR* allele identifies a putative oxidative stress regulon. Microbiology 152:2599–2609. https://doi.org/10.1099/mic.0.28996-0.
57. Ouyang Z, He M, Oman T, Yang XF, Norgard MV. 2009. A manganese transporter, BB0219 (BmtA), is required for virulence by the Lyme disease spirochete, *Borrelia burgdorferi*. Proc Natl Acad Sci U S A 106:3449–3454. https://doi.org/10.1073/pnas.0812999106.
58. Whitehouse CA, Williams LR, Austin FE. 1997. Identification of superoxide dismutase activity in *Borrelia burgdorferi*. Infect Immun 65:4865–4868.
59. Troxell B, Xu H, Yang XF. 2012. *Borrelia burgdorferi*, a pathogen that lacks iron, encodes manganese-dependent superoxide dismutase essential for resistance to streptonigrin. J Biol Chem 287:19284–19293. https://doi.org/10.1074/jbc.M112.344903.
60. Aguirre JD, Clark HM, McIlvin M, Vazquez C, Palmere SL, Grab DJ, Seshu J, Hart PJ, Saito M, Culotta VC. 2013. A manganese-rich environment supports superoxide dismutase activity in a Lyme disease pathogen, Borrelia burgdorferi. J Biol Chem 288:8468–8478. https://doi.org/10.1074/jbc.M112.433540.
61. Getz EB, Xiao M, Chakrabarty T, Cooke R, Selvin PR. 1999. A comparison between the sulfhydryl reductants tris(2-carboxyethyl)phosphine and dithiothreitol for use in protein biochemistry. Anal Biochem 273:73–80. https://doi.org/10.1006/abio.1999.4203.
62. Krężel A, Lesniak W, Jezowska-Bojczuk M, Mlynarz P, Brasun J, Kozlowski H, Bal W. 2001. Coordination of heavy metals by dithiothreitol, a commonly used thiol group protectant. J Inorg Biochem 84:77–88. https://doi.org/10.1016/S0162-0134(00)00212-9.
63. Laemmli UK. 1970. Cleavage of structural proteins during the assembly of the head of bacteriophage T4. Nature 227:680–685. https://doi.org/10.1038/227680a0.
64. Barbour AG, Hayes SF, Heiland RA, Schrumpf ME, Tessier SL. 1986. A Borrelia-specific monoclonal antibody binds to a flagellar epitope. Infect Immun 52:549–554.